Cement and Concrete Research 41 (2011) 1185–1195

Contents lists available at ScienceDirect

Cement and Concrete Research

journal homepage: http://ees.elsevier.com/CEMCON/default.asp

Wavelet-based analysis of ultrasonic longitudinal and transverse pulses in cement-based materials

Carnot Leal Nogueira *

Civil Engineering Department, Federal University of Pernambuco (UFPE), Brazil

ARTICLE INFO

Article history:
Received 21 January 2011
Accepted 22 July 2011

Keywords:
Concrete (E)
Mortar (E)
Mechanical properties (C)
Aggregate (D)
Microstructure (D)

ABSTRACT

Ultrasonic pulse velocity has been used for decades to detect localized damage and to estimate concrete properties. More recent applications aim at diffuse damage characterization, such as environmental and mechanical damage. In most applications the methodology to calculate pulse speed is a very important issue. This work, applying continuous wavelet transform (CWT) to construct time-frequency signal representations, calculates frequency-dependent velocity of longitudinal and transverse ultrasonic pulses using wavelet scales. The method is applied to a total of 14 specimens of 5 different mixes and frequency-dependent velocities are calculated using four wavelet families. The CWT capability to decompose the inquiring pulse spectrum and analyze phase velocities is discussed with regard to wavelet, pulse type, and mixture. Frequency-dependent velocity of longitudinal pulses at lower frequencies (from 100 kHz up to 250 kHz) was proven to be much more sensitive to mix proportions than transverse pulses.

1. Introduction and research significance

One of the first publications about the application of ultrasonic testing to concrete appeared in 1949 [1]. The authors conducted a research about detecting and analyzing cracks on concrete structures, and also studied distributed damage due to freeze and thaw cycles. In the same research ultrasound was used to estimate concrete quality. The study was largely based upon longitudinal pulse velocity.

More than 60 years have passed since that study was published and due to a great development of ultrasonic equipment (pulser/receiver circuitry, oscilloscopes, and transducers) and also due to the great progress in analysis methods (scientific computing, mathematical and numerical methods) ultrasound has established itself as one of the most widely used nondestructive techniques for concrete inspection in Civil Engineering. Ultrasound is a relatively cheap, very safe, and reliable real-time method. Furthermore, the portability of the currently available equipments makes ultrasonic testing adequate for the analysis of structures while in use. In addition to these advantages, ultrasound delivers information about pulse velocity, attenuation and amplitude. The interrelations of these three parameters are of great importance to study non-homogeneous media such as concrete and other cement-based materials.

The inhomogeneous nature of concrete, due to its constitutive *phases* (grain-size distribution of the aggregates, matrix, inclusions), and also diffuse damage (due to mechanical loading, freeze-thaw cycles, alkali-aggregate reaction, and sulfate attack, for example) have both an enormous influence in ultrasonic pulse behavior in concrete. As a consequence of this inhomogeneous, dispersive and granular nature of concrete, interactions between velocity, attenuation and frequency cannot be neglected, and the interrelations of these three parameters are even more important when some specific aspect – such as stress-induced anisotropy (compressive loading in a preferred direction induces microcrack formation *in the same* direction) – is under analysis. This issue has been – unfortunately – often neglected by most researchers in the field of concrete ultrasonic investigation.

The relevance of the interaction between velocity, attenuation and frequency can be clearly seen even in very simple ultrasonic application to concrete inspection such as ultrasonic pulse velocity measurement. This widely-used application, which is a standard test method in several countries (e.g., in the USA, ASTM C597-02; in Europe, BS EN 12504–4:2004; in England, BSI 98/105795; in Germany, DIN EN 12504–4; in Brazil, ABNT NBR 8802:1995), can be used to detect voids and honeycombs, to estimate compressive strength, and to analyze cracks. Nonetheless, in order to measuring the velocity – for example, in methods such as zero-crossing – the changes in pulse shape are *not* taken into account. This fact is illustrated in Fig. 1. The figure depicts two ultrasonic pulses: the one on top represents a transducer–transducer pulse (transducer surfaces were connected by a thin layer of couplant) while the pulse at the bottom represents a through-concrete pulse (transducers were connected to the parallel surfaces of the concrete specimens with couplant). Both pulses are represented in time domain: time at horizontal axis was measured at a sampling rate of $10^7\ s^{-1}$. Besides the considerable amplitude decay, the pulse suffers a dramatic change in its shape. Due to the pulse-shape

* Rua Zezito Costa Rego, 246, CDU, 50.740-010, Recife/PE, Brazil. Tel.: +55 81 9961 6357; fax: +55 81 3427 3796.
E-mail address: carnot@tce.pe.gov.br.

0008-8846/$ – see front matter
doi:10.1016/j.cemconres.2011.07.008

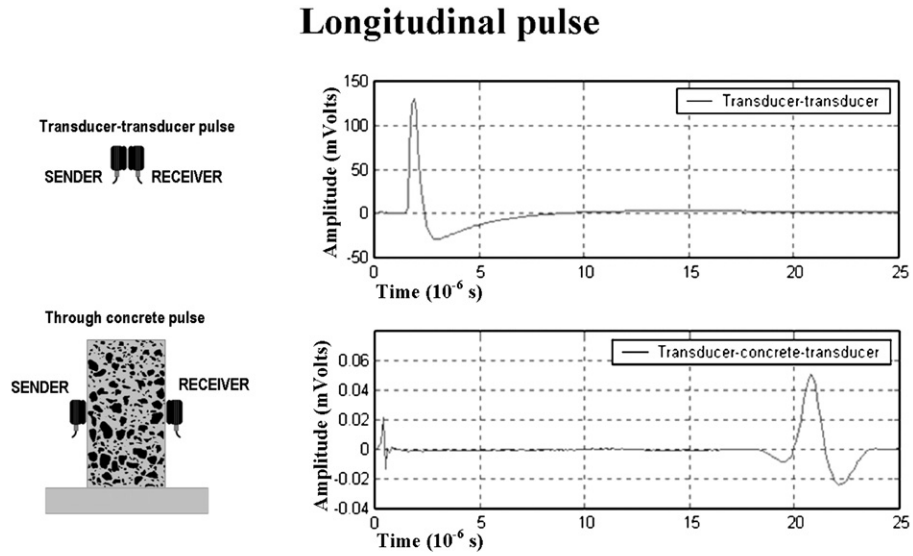

Fig. 1. Ultrasonic pulse aspect in time domain: transducer–transducer pulse (top) and pulse transmitted through concrete (bottom).

change (which is a consequence of frequency-dependent attenuation) any pulse velocity measurement, such as the zero-crossing method, can be greatly affected.

Fig. 2 shows Fourier transforms of pulses illustrated in Fig. 1. The signals are comprised of several frequencies, ranging – approximately – from $2 \cdot 10^4$ to $5 \cdot 10^6$ Hz. It can be observed that propagation through concrete greatly affects frequency contents. Normalized amplitude of through-concrete signal shows that some frequencies are cut due to total attenuation (above 10^6 Hz). Furthermore, frequency curve is no longer smooth and the relative values of the amplitudes change greatly (for example, while in the top plot the amplitudes of the frequencies 10^5 Hz and $2 \cdot 10^5$ Hz are both close to unity, in the through-concrete pulse the amplitude corresponding to 10^5 Hz is nearly half of the amplitude at $2 \cdot 10^5$ Hz). As a result, the frequency spectrum, as a whole, greatly changes with the propagation. Although frequency-based information can be used to detect environmental damage [2] and estimate grain-size distribution [3], *undesired frequency content changes* distort the pulses and spuriously influence velocity readings. The implications of pulse shape distortion due to attenuation of specific frequencies can be analyzed with continuous wavelet transform (CWT).

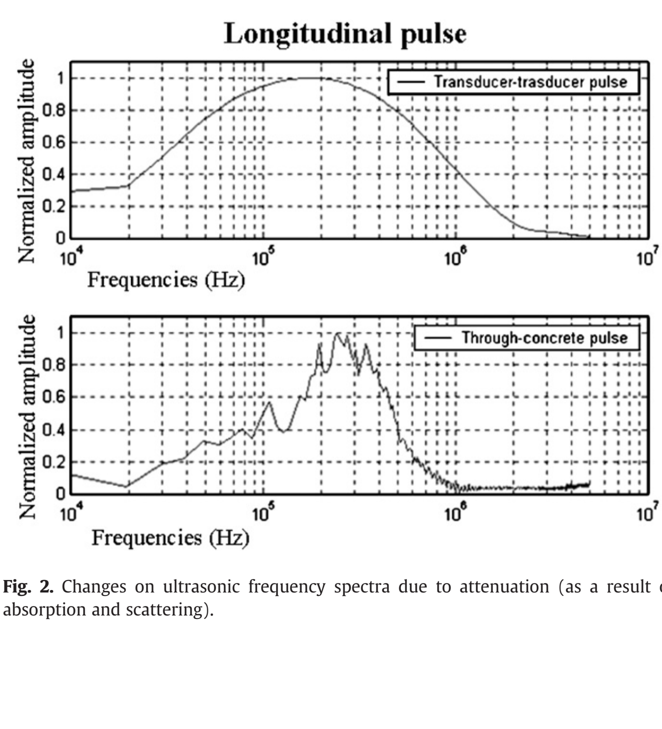

Fig. 2. Changes on ultrasonic frequency spectra due to attenuation (as a result of absorption and scattering).

2. Continuous wavelet transform for velocity measurements

With the application of continuous wavelet transform frequency-based information from broadband ultrasonic pulses can be extracted. The method allows monitoring the behavior of specific frequencies of interest while propagating in dispersive medium [3,4]. The advantages of CWT can be easily understood when compared to Fourier transform or windowed Fourier transform.

Fourier transform of a function allows one to calculate the signal magnitude of a specified frequency. While frequency determination in the Fourier transform is precise it implies a loss of time information [4]. As a consequence Fourier transform does not capture transient phenomena as those that take place during ultrasonic wave propagation in dispersive media such as concrete and mortar. This inability to capture transient phenomena makes Fourier transform inadequate for frequency analysis in time domain. To overcome the inadequacy of Fourier transform for the analysis of transient phenomena, a *compactly supported* version of it was created. The technique – called windowed Fourier transform or short-time Fourier transform (STFT) – was initially proposed by Gabor in 1946 in an article on data transmission [5]. The STFT consists on multiplying the original signal by a compactly supported function and calculating the Fourier transform of the product. Time information can be obtained by translating the multiplying function in the time domain. Although Gabor's proposal was based on a Gaussian windowing function, which is not a compactly supported function, the technique allowed some compromise between time and frequency in the signal analysis. A shortcoming of the STFT method is the *fixed size* of the windowing functions: once a particular windowing function is chosen that window is the same for all frequencies. This renders the technique not adequate for the analysis of signals whose spectra range from very low to very high frequencies. In addition, some phenomena, like discontinuities in the signal, can only be captured with the use of very short basis functions [6]. In order to extract detailed and reliable information from wide-spectrum signals one needs to have both high- and low-frequency analyzing windows.

Transient frequency analysis of ultrasonic signals can be performed with the application of functions that can be *translated* and that allow *changes in scale*. With translations one can precisely determine *when* phenomena occur (*localize* them in time), while with changes in scale phenomena of varying frequency range can be captured. Translation and scaling are inherent characteristics of CWT, whose properties are based upon translation and scaling operations of the *mother wavelet* adopted in the analysis [7]:

$$\psi_{(a,b)}(x) = \frac{1}{\sqrt{a}}\psi\left(\frac{x-b}{a}\right). \quad (1)$$

In the above equation parameter a allows *scaling* operations to be performed, while parameter b is used for translations. Using these two parameters similarity coefficients $C_{a,b}$ can be defined using the integral [3,7]:

$$C_{a,b} = \int_{-\infty}^{+\infty} s(t)\frac{1}{\sqrt{a}}\psi\left(\frac{t-b}{a}\right)dt. \quad (2)$$

Coefficients C calculated with the above equation can be readily associated to any phase frequency of the pulse, since the product of the *scale* used and the *frequency analyzed* is a constant which depends upon the wavelet adopted in the analysis only. The pulse energy corresponding to a specific scale a can be calculated using [8]:

$$E_a = \sum_{n=0}^{1024} \left|C_{a,n}\right|^2 \quad (3)$$

where 1024 (2^{10}) is the total number of averaged ultrasonic pulse readings used in the experiments. Propagating speed of that specific scale a (that corresponds to a specific frequency) can be calculated using the first moment of energy:

$$t_a = \frac{\sum_{n=0}^{1024} n\left|C_{a,n}\right|^2}{\sum_{n=0}^{1024} \left|C_{a,n}\right|^2}. \quad (4)$$

With the above equations the *time* (t_a) needed for a *specific frequency* of a broadband pulse to cross a dispersive media can be computed. This is due to the fact that parameter a allows *scaling* and therefore each t_a can be computed for a specific scale associated to one frequency only. The same procedure can be used to calculate frequency-dependent attenuation which has been successfully used to estimate grain-size distribution [3].

It is important to emphasize that the *wavelet type* can be used as a parameter that can be adjusted in the analysis, in such a way that frequency-dependent velocity (and also frequency-dependent attenuation) can be calculated for each wavelet type used. Since the similarity between the propagating ultrasonic pulse and the inquiring wavelet (Eq. (1)) plays an important role in the pulse energy and momentum calculated with Eqs. (3) and (4), the wavelet chosen for the analysis strongly influences the results. Wavelets that are similar in shape to the ultrasonic pulses lead to more consistent results. Fig. 3 shows five wavelet families. Comparing the wavelet shape and the ultrasonic pulse aspect (Fig. 1) one can select adequate wavelet families. Since pulse shape depends upon the pulse generator circuitry, transducers and coupling, and also upon concrete type and properties, the capability of changing the wavelet type (*or the wavelet order in the same wavelet family*) is very useful.

Wavelet analysis, as above described, corresponds to size-varying tiles, tiles whose sides form *time-frequency cells*. The side length of the tiles varies according to the level of scaling and the tiles can be displaced along the time axis with translations (and this varying size of the cells, as mentioned above, is the main advantage when wavelets are compared to the widowed Fourier approach). The scaling operation of a wavelet leads to an increase in the value of its frequency by a factor of $2^{\,j}$, with j = 0, 1, 2… n, concomitantly the support (interval of definition) of the wavelet is contracted by the same factor $2^{\,j}$. The product of the *intervals of definition* (supporting interval) of the wavelet in frequency domain and time domain remains constant but *cannot be arbitrarily small.* The lower bound for the area defined by that product (*time-frequency tile area*) is given by the Heisenberg uncertainty principle. This famous principle was formulated in 1926 in the context of quantum mechanics providing limits for the simultaneous determination of free particle position and momentum. In wavelet analysis the uncertainty principle limits simultaneous definition of functions in *both* time and frequency domains. Applications and a demonstration of the Heisenberg uncertainty principle in the context of wavelet analysis can be found in Strang and Nguyen [9] and Mallat [8].

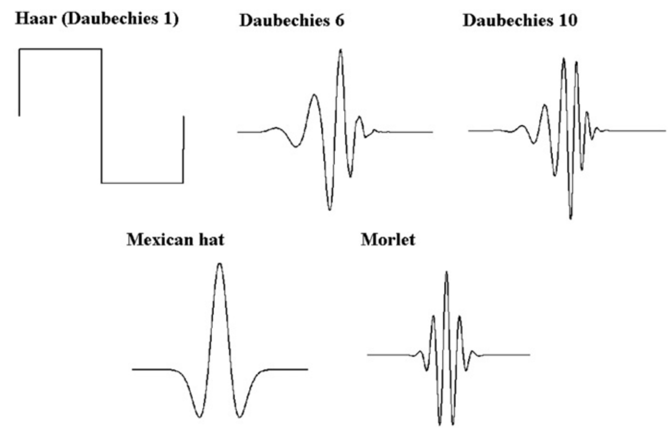

Fig. 3. Wavelet families.

Wavelet analysis of multi-phase pulses can be performed as shown in Fig. 4. The top plot shows the ultrasonic pulse in time domain. Although not readily distinguishable in time domain, pulse is composed by a slow decaying phase (its amplitude has a linear decrease) and by a faster phase with cubical increase in amplitude. The signal is described by the following equation:

$$s[x] = \cos\left[2\cdot10^5\cdot2\pi\frac{x}{SR}\right]\left[1-\frac{x}{1024}\right] + \cos\left[8\cdot10^5\cdot2\pi\frac{x}{SR}\right]\left[\frac{x}{1024}\right]^3 \quad (5)$$

with $x = 0, 1, 2, \ldots, 1024$ and $SR = 10$ MHz.

Fourier transform of the signal is represented below the time domain plot, peak frequencies can be easily identified at $f = 2\cdot10^5$ Hz and $f = 8\cdot10^5$ Hz. As one can see both peaks show smooth decrease at the sides of the maxima. While both peaks can be clearly identified, no information about the transient behavior of the pulse can be observed: one *cannot* observe the decaying phase nor the increasing one. The third plot in Fig. 4, below the Fourier-based frequency spectrum curve, is the wavelet-based time-frequency representation of the pulse. Time is shown in the abscissa axis and scales are depicted in the ordinate axis (*wavelet scales*), scales vary from s = 1 to s = 80. The central frequency of the Daubechies 6 wavelet used in the analysis is $\eta = 8\cdot10^6$ Hz, and equation $s\cdot f = \eta$ can be used to relate frequencies f to scales s [8,3]. Thus scales corresponding to the peak frequencies can be calculated as s = 40 ($f = 2\cdot10^5$ Hz) and s = 10 ($f = 8\cdot10^5$ Hz). In the CWT-based time-frequency domain *interference fringes* can be observed in shades of white at the left side of the diagram, as well as in the right side at the lower part of the diagram. The *interference fringes* are a result of the varying similarity coefficient values $C_{a,b}$ calculated from Eq. (2). Since the – *stretched* and *translated* – Daubechies 6 wavelet *pulses* (Fig. 3) interact with the *analyzed pulse* (Eq. (5)), in-phase and out-of-phase regions are created and the values of the similarity coefficients vary.

In the two last plots of Fig. 4 the decaying linear pattern of the slower phase amplitude (scale s = 40, frequency $f = 2\cdot10^5$ Hz), as well as the amplitude cubic increase of the higher phase (scale s = 10,

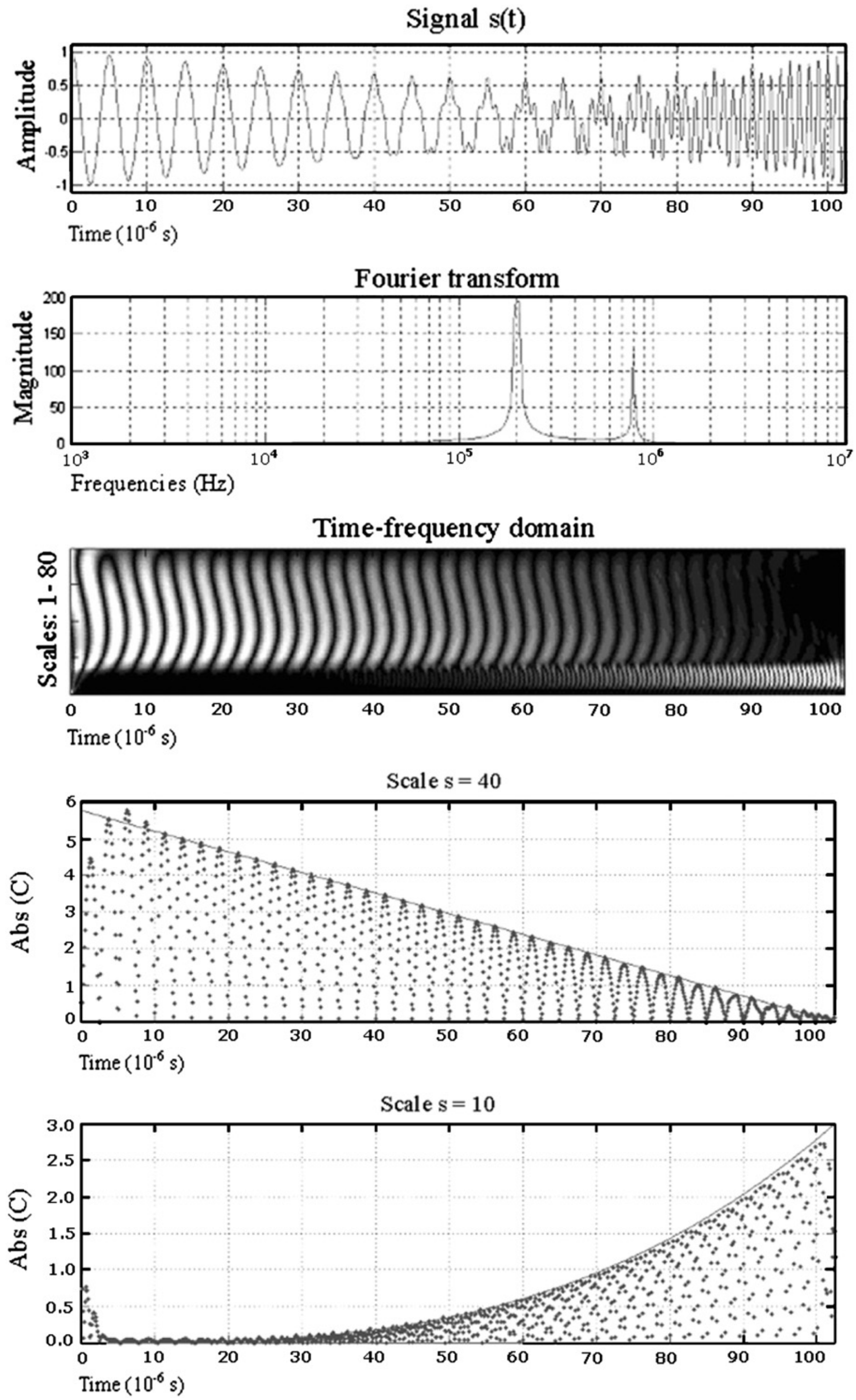

Fig. 4. Composed signal: time domain, Fourier representation and time-frequency domain (top). Absolute values of the wavelet coefficients at scales s = 40 ($f = 2 \cdot 10^5$ Hz) and s = 10 ($f = 8 \cdot 10^5$ Hz) show the transient nature of specific frequencies (bottom).

frequency $f = 8 \cdot 10^5$ Hz), is depicted. The transient nature of the pulse behavior can, therefore, be analyzed with regard to each component frequency if one inspects each scale individually. Since the energy of each scale can be computed from Eq. (3), for each scale a one can compute the first moment (*time* t_a) from Eq. (4) of the through-concrete pulses and then compute the frequency-dependent (*scale-dependent*) velocities. In the following, using 4 different wavelet families, frequency-dependent velocities are calculated for longitudinal and transverse ultrasonic pulses propagating in concrete (three mix designs), mortar and hardened cement paste.

3. Mix design and experimental program

As emphasized in the Introduction, issues related the velocity measurements of broadband pulses propagating in dispersive media, such as cement-based materials, are very important for more sophisticated applications of ultrasonic methods. To validate the analysis above described, which allows frequency-wise velocity measurements of pulses, an experimental program based upon CWT time-frequency representations was applied to ultrasonic pulses propagating through three concretes, mortar, and hardened cement paste. Type 1 Portland cement was used for all mixes. Specimens were cast in steel molds for 24 h and then stripped and kept in the fog room for 28 days. Specimens were then placed in ambient conditions for at least 1 day before ultrasonic pulses were applied. All specimens of each mix were cast from the same batch. Specimens were prismatic with dimensions 76.2 × 76.2 × 152.4 mm, two opposite 76.2 × 152.4 mm faces were carefully ground for better attachment of the transducers and to ensure parallelism of the surfaces. To transmit and receive the ultrasonic signals, two pairs of corresponding transducers (a pair of longitudinal and a pair of transverse wave probes) were precisely aligned on the opposite ground sides (as shown in Fig. 5). Concrete mix aggregates were proportioned according to ASTM standard grading requirements, the average sizes of the aggregates used in the three concrete mixes were: coarse concrete (mix A) — 4.75 mm, medium concrete (mix B) — 2.36 mm, and fine concrete (mix C) — 1.77 mm. Coarse and fine aggregate proportions, water/cement ratio, as well as compressive strength at 28 days (an average value of three crushed specimens) for all mixes used can be found in Table 1.

The ultrasonic instrumentation equipment consists of four basic parts. The first part is the piezoelectric transducers. All 4 transducers used were manufactured by Panametrics and have a diameter of 25.4 mm. Longitudinal wave transducers operate at a nominal frequency of 500 kHz (model V101-RB), while the transverse wave ones operate nominally at 250 kHz (model V150-RB). The transducers provide heavily damped broadband performance, producing improved signal-to-noise ratio in attenuating and scattering materials. The probes were connected to the ground sides of the specimen with a thin layer of couplant. The second part is the pulse/receiver card manufactured Matec Instruments (SR-9000). Gain, low-pass and high-pass filters can be controlled with the software provided by the manufacturer. Since the card allows only one output for the transmitter and one input for the receiver, a switching box – the third part of the equipment – was needed to control which pair of transducers was operating. The last piece of ultrasonic equipment is the oscilloscope card that converts the data received to digital form and saves the files for the analysis. A CompuScope CS-1012 card capable of a sampling frequency of 10 MHz in dual channel mode was used.

The two last columns at the right side of Table 1 show the average values of the longitudinal and transverse pulse speeds computed with the *zero-crossing* method. The velocities, therefore, were computed based upon the *difference* between the zero-crossing *time positions* of

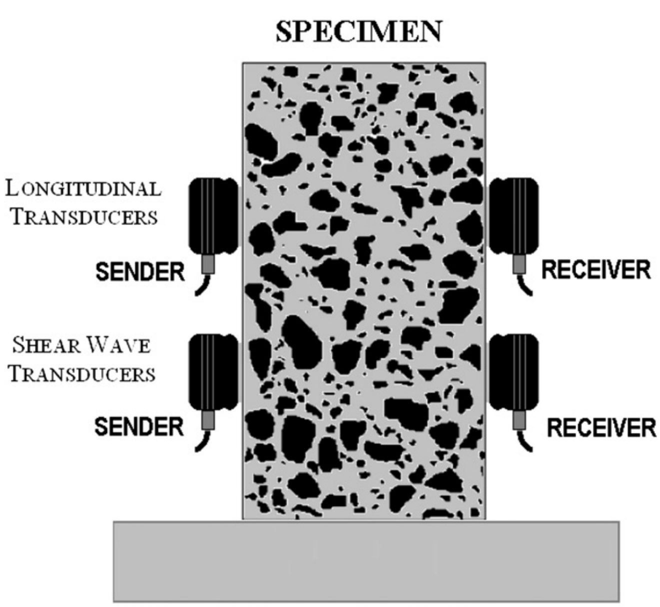

Fig. 5. Experimental setup.

Table 1
Mix design and average values of compressive strength, longitudinal and transverse wave velocities.

Mix	Mixture proportions[a] C:CA:FA (W/C)	Compressive strength[b] (MPa)	Longitudinal wave velocity (m/s)	Transverse wave velocity (m/s)
Concrete A	1:1.57:2.01 (0.55)	26.98	3983	2361
Concrete B	1:0.71:2.86 (0.55)	29.99	3920	2401
Concrete C	1:0.00:3.60 (0.55)	26.74	3898	2369
Hardened cement paste	1:0:0 (0.5)	19.99	3525	1820
Mortar	1:0:1 (0.5)	22.40	3850	2210

[a] Fractions in weight: C—cement, CA—coarse aggregate, FA—fine aggregate (≤4.75 mm), W/C-water/cement ratio.
[b] Average values of three tests for concretes and mortar and two tests for hardened cement paste. Compression tests were performed at 28 days.

the transducer–transducer and the through-concrete pulses shown on top and bottom of Fig. 1, respectively. On the top plot of Fig. 1, transducer–transducer pulse, the zero position can be identified right after the voltage spike (peak amplitude) at, approximately, $t = 2.5 \cdot 10^{-6}$ s. The bottom plot shows the (attenuated and greatly modified) through-concrete pulse, in the figure zero crossing of the main oscillation (the total amplitude of the main oscillation varies from about −0.025 mV to 0.050 mV) that occurs at approximately $t = 22 \cdot 10^{-6}$ s. Therefore, using the *zero-crossing* approach, the pulse takes $22 \cdot 10^{-6}$–$2.5 \cdot 10^{-6} = 19.5 \cdot 10^{-6}$ s to cross 76.2 mm of concrete, this means that the pulse propagated 0.0762 m in $19.5 \cdot 10^{-6}$ s, resulting in a velocity of 3908 m/s. It should be emphasized that the values abovementioned are explanatory only, adopted only to illustrate the procedure. In order to calculate the velocity values presented in Table 1, the exact time of crossing was computed with an interpolation of the last positive and first negative signal reading. Furthermore, digital equipment was used to measure the propagating distance between the opposite ground faces of the specimens (which was always a little less than 76.2 mm due to grinding). Since the whole pulse with the complete frequency spectrum is considered (Fig. 2), the computed velocities using the above described *zero-crossing method* are group velocities.

4. Frequency-dependent velocity and attenuation of ultrasonic pulses

No abundant information exists about ultrasonic longitudinal phase-velocity behavior in granular media, and even less about longitudinal *and transverse* wave pulse- and phase-velocities propagating in granular, inhomogeneous, dispersive, non-metallic cement-based materials. It is, nonetheless, well known that *longitudinal* ultrasonic wave attenuation while propagating in dispersive media depends upon absorption and scattering [10,11] and both phenomena depends upon pulse frequency [11–14]. While the dependency of absorption and frequency can be taken as linear, scattering depends upon the relation between grain-size D and wavelength λ. The dependency between wavelength and grain size then leads to the definition of scattering regions, which are three (depending upon the ratio λ/D): Rayleigh, stochastic and diffusive, each region following particular laws regarding attenuation due to scattering [15–17].

The complexities related to high frequency ultrasound – above 100 kHz – have been noticed by some researchers of wave propagation in cement-based materials [18–20]. But although difficulties exist, in order to obtain grain-size information or to assess microcrack formation in concrete, wavelengths whose sizes are comparable to grain diameters and microcrack width have to be applied. Assuming a longitudinal wave velocity $V_L = 4000$ m/s (which is a typical value for good concrete) and considering one is interested in getting information in the range [0.008 m, 0.04 m] – spanning, therefore, from coarse aggregate (with a few centimeters) to fine aggregate or microcrack size (with a few millimeters) – the frequency range used has to be in the interval $f \in [10^5\,\mathrm{Hz},\ 5 \cdot 10^5\,\mathrm{Hz}]$ (*frequency* multiplied by the *wavelength* gives the *velocity*). If one is interested in analyzing smaller grain-sizes or microcracks, frequencies even higher have to be applied. It can be concluded that *high frequency ultrasound* is necessary for more sophisticated and precise techniques to be applied in diffuse damage or grain-size inspection of cement-based materials.

During the last decades some of the results obtained in research programs about high frequency ultrasound on concrete have not been consistent. An extensive analysis of attenuation mechanisms of ultrasonic waves propagating in concrete led to the conclusion that scattering plays the main role in attenuation [10]. Contradicting that conclusion, more recent research – which used Rayleigh surface waves – concluded that absorption is the main attenuating process [11]. For several reasons, attenuation dependency upon frequency of pulses propagating in concrete, rather than *velocity dependency upon frequency*, has been the main concern of ultrasonic investigation. Gaydecki et al. using partitioned ultrasonic signal analysis (in the study *discrete windows in time domain* were applied), showed that it is possible to obtain information about grain-size distribution of the concrete aggregate phase [10]. Owino and Jacobs used laser ultrasound to investigate material frequency dependent attenuation of Rayleigh waves. In the study it was emphasized that it is possible to characterize the microstructure of cement-based materials from ultrasonic *attenuation* losses [12]. The same authors analyzed the effect of *aggregate size* on the attenuation of Rayleigh surface waves in cement-based materials and concluded that *absorption losses* play a major role in the attenuation, while *scattering losses* are negligible [9]. Becker, Jacobs and Qu applied ultrasound in the analysis of hardened cement-paste matrix with glass bead inclusions. In the results qualitative trends in the scattering losses were observed, indicating the possibility of ultrasonic characterization of distributed *damage* in cement-base materials [21].

Mechanical damage detection with ultrasonic longitudinal pulse velocity and attenuation, although applied and studied for decades [4,14,20,21], still challenges researchers. In a recent study conducted by Shah and Hirose damage on concrete specimens under several step loads was evaluated with a nonlinear ultrasonic testing technique [22]. Results showed that attenuation is more sensitive to damage than velocity and that velocity is not sensitive to damage until 60% of concrete compressive strength is reached.

Some publications that directly address attenuation of high-frequency ultrasound propagating in cement-based materials also deserve attention for introducing novel processing methods. In a work published in 2000, Popovics et al. used Gaussian filters that do split ultrasonic frequency spectrum and improve signal-noise ratio [23]. The signal is partitioned in frequency bands (windows) and reassembled, in such a way that – with noise suppression algorithms – scatter noise is canceled out. The potential of the applied technique to detect internal defects with high-frequency ultrasound was demonstrated. Another novel approach – frequency-dependent amplitude attenuation characteristics technique (FACT) – was introduced in 2006 [24]. The results showed that an *attenuation function* can be used to detect damage (a volume fraction of Styrofoam spheres) with ultrasonic longitudinal pulses up to 1 MHz. Results also demonstrated that longitudinal wave velocity is far less sensitive to damage than amplitude attenuation.

The effect of artificially introduced *damage* (plate-shaped plastic inclusions) on ultrasonic longitudinal wave propagation in cement-based materials was analyzed – with narrow-band pulses of several different frequencies – by Aggelis and Shiotani [25]. For the maximum inclusion content used (10%), it was observed a remarkable increase in velocity as the frequency is elevated. The authors conclude that narrow band signals are adequate to reveal velocity dispersion caused by inhomogeneity and also that velocity measurements at different frequencies can be used to assess damage.

It is also worth emphasizing that ultrasonic longitudinal wave velocity has also been used to monitor setting and hardening of concrete and mortar. De Belie, Grosse and coworkers have demonstrated that both velocity and frequency deliver information about setting and hardening processes of cement-based materials [26,27]. This interesting new application of ultrasonic testing allows obtaining microstructure change information via well known wave propagation parameters, such as pulse velocity and frequency contents.

One should notice that, although *frequency-dependent attenuation* directly affects *velocity*, and although pulse *velocity* can be directly related to propagating medium properties *or to the degradation of those properties* [2,4,18–20], only in recent years more sophisticated research programs address *frequency-dependent attenuation* influence on *velocity* [3,22,24]. In an interesting work by Philippidis and Aggelis, narrow band longitudinal transducers with several different frequencies were applied to concrete and mortar with varying water–cement ratio and specimen geometry [13]. The results addressed the variation of longitudinal pulse velocity with frequency: a *tendency to a constant, uniform value of the pulse velocity can be observed as the frequency increases* (spectra up to 1.0 MHz were considered). This behavior occurs regardless of varying water/cement ratio, aggregate size, specimen size and geometry, and propagating direction. Another recent research used CWT-based analysis of longitudinal high frequency ultrasonic pulses to estimate grain-size distribution in cement-based materials [3]. The tests conducted proved that with a single pair of broadband high-frequency probes estimates of grain-size distribution in concrete can be obtained.

The lack of information about high frequency ultrasound applied to concrete (there is almost no published information about transverse waves), and the complexity of the phenomena related to attenuation (scattering and absorption) at high frequencies are two issues that should be taken into account in the study of grain-size or microcracking in cement-based materials with *velocity* measurements. In addition, the number of parameters that directly influence propagation of ultrasound – influencing *both attenuation and velocity* – in cement-based materials (grain-size distribution, water/cement ratio, compressive strength, cement type, additives, microcracking, entrained air etc.) further complicates the scenario. In the following the results obtained with the application of CWT to measure longitudinal and transverse ultrasonic wave *phase* velocities as functions of the pulse-composing frequencies are presented and discussed.

5. Results and discussion

Four wavelet families, namely: Haar (Daubechies 1), Mexican hat, Daubechies 6, and Daubechies 10 (Fig. 3) were used to calculate – based on formulae of Eqs. (3) and (4) – the frequency-dependent velocities of all five mixes (Table 1). Fig. 5 shows the experimental setup. The results are presented in Figs. 6–9. Each figure shows the frequency-dependent longitudinal and transverse wave velocities of each mix: upper plots show the results for concrete mixes, while the ones at the bottom show the velocities for mortar and hardened cement paste. Due to attenuation, pulse spectrum was narrowed down from the range presented in Fig. 2 into a smaller interval, rendering a useful spectrum from 10^5 Hz up to $5 \cdot 10^5$ Hz. This interval – considering longitudinal and transverse pulse velocities $V_L = 4000$ m/s and $V_T = 2400$ m/s, respectively (Table 1) – correspond to wavelength ranges $\lambda_T \in [4.8\ \mathrm{mm},\ 24\ \mathrm{mm}]$ and $\lambda_L \in [8\ \mathrm{mm},\ 40\ \mathrm{mm}]$. Wavelengths considered are, therefore, comparable in size to the larger aggregates in concrete mixes (*stochastic region*) and larger than fine aggregates and cement particles (*Rayleigh region*). For each wavelet and each mix, time-frequency diagrams – such as the one presented in Fig. 4 – were constructed and the first moment of energy (Eq. (4)) was calculated for each scale. For each scale in the vertical axis the time delay that corresponds to energy concentrations along the time axis was then computed. A frequency-based (or, equivalently, a *scale-based*)

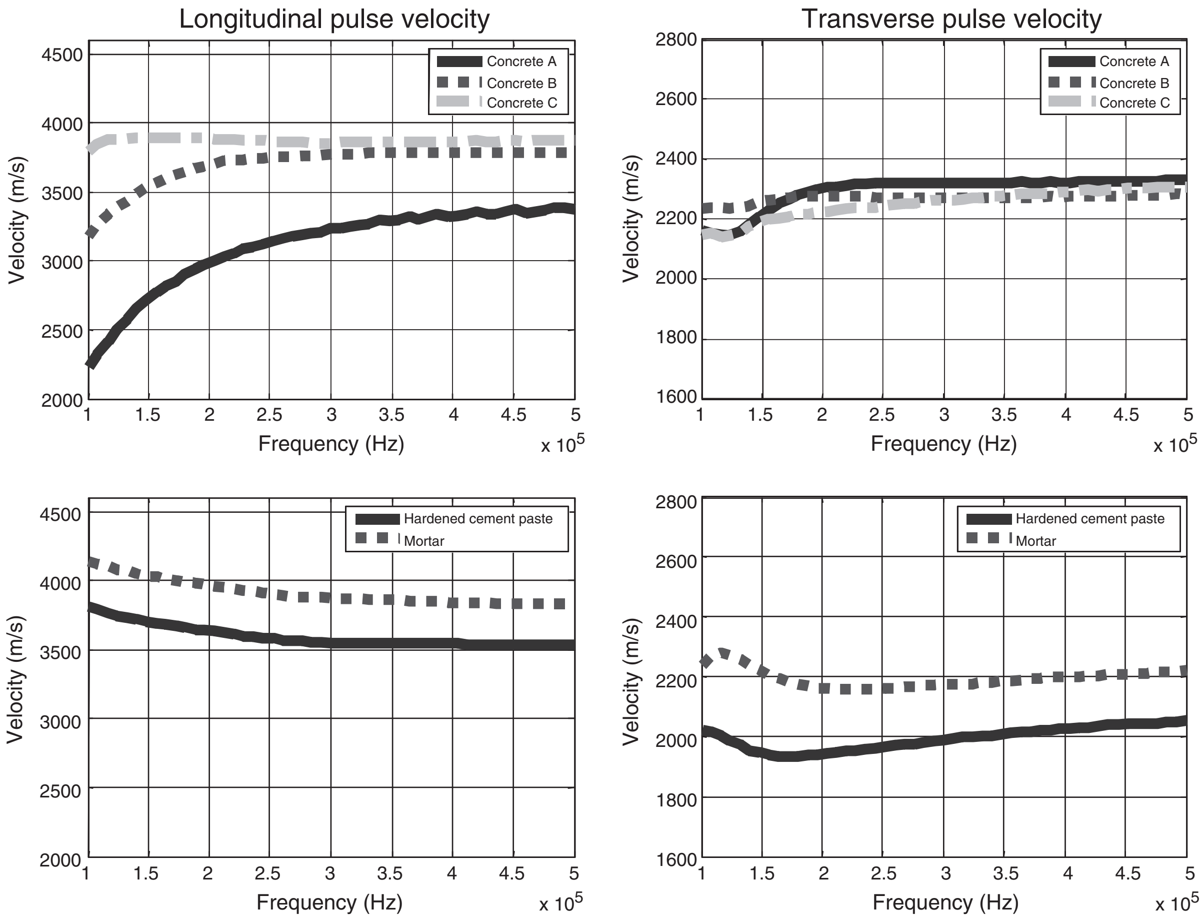

Fig. 6. Frequency-dependent velocity of longitudinal and transverse pulses based on Haar wavelets.

comparison of the transducer–transducer and the through-concrete pulses (Fig. 1) allows the velocities to be calculated as a function of any given frequency in the range $[10^5, 5 \cdot 10^5 \text{ Hz}]$.

Velocities, in the vertical axis, are shown as a function of the frequencies at the ordinate axis. In each of the frequency-dependent velocity figures – Figs. 6–9 – ten curves are depicted. The plots at the left-hand side show the results for the longitudinal pulse velocities, while the ones at the right-hand side depict the transverse wave velocities. The two plots at the top of each figure – with three curves each – show the behavior of the 3 concrete mixes (concrete A — coarse concrete — solid line, concrete B — medium concrete — dotted line, concrete C — fine concrete — dash-dot line), while each of the plots at the bottom shows two curves only: hardened cement paste — solid line, mortar — dotted line. Each curve was computed from the mean values obtained from all specimens made from each material (3 specimens of each concrete type and mortar, and 2 specimens of hardened cement paste — total of 14 specimens). Although mean values were used, it is worthy to emphasize that the curves for each material type follow similar patterns.

Results display velocity values which are not always close to the *zero-crossing-based* velocities shown on Table 1. This is due to changes in frequency spectrum and in pulse shape while propagating through the specimens (Fig. 1). Frequency-based *phase* values are intrinsically different from *group* velocities calculated from *zero-crossing*, which can be considered a *mean* value of the frequency subset that traveled through the whole propagating path and reached the receiving transducer. In the analysis of the results, the following aspects are taken into account: (i) the wavelet used to calculate the velocities, (ii) the pulse type used, either longitudinal or transverse, and (iii) the coarseness of the mix.

5.1. Wavelet family

With regard to the wavelet used, comparing the four pictures, the results obtained for mortar and hardened cement paste, for both transverse and longitudinal waves, have velocity curves that display the same general trends not depending upon the wavelet used. This indicates that less inhomogeneous and less dispersive mixes are not very sensitive to the wavelet used in the analysis. On the other hand, concrete mixes showed – for both wave types – a behavior that strongly depends upon the wavelet. The transverse pulse velocity curves obtained for concrete mixes with Daubechies 6 and Daubechies 10 wavelets (Figs. 8 and 9) display a spurious increase as the frequency tends to the upper limit $f = 5 \cdot 10^5$ Hz. This is a consequence of an interaction of the *faster* wavelets (these two wavelets oscillate faster than the Haar and Mexican hat — Fig. 3) with noise at the strongly attenuated higher frequencies of the transverse pulses (nominal frequency of the transverse wave probes $f = 250$ kHz is half of the longitudinal wave pressure transducers nominal frequency). As a result, the *faster* wavelets *read* the noise at the right-hand side of the spectrum as pulse components. This spurious behavior helps emphasize the fact that the *wavelet* used must be considered as a *parameter* for wavelet analysis of ultrasonic pulses. When the wavelet family allows one to *vary* the *order of the wavelet* chosen, the *order* itself can be taken as a parameter. This is occurs with wavelets such as Symlets, Coiflets, and – as abovementioned – Daubechies wavelets (one can chose order 1 — Daubechies 1, which is the Haar wavelet, order 6, order 10, or order 20, in a growing sequence of frequencies). An adequate wavelet can help strengthen the useful signal information, while a *wrong* or *inappropriate* type may tend to hide the useful information

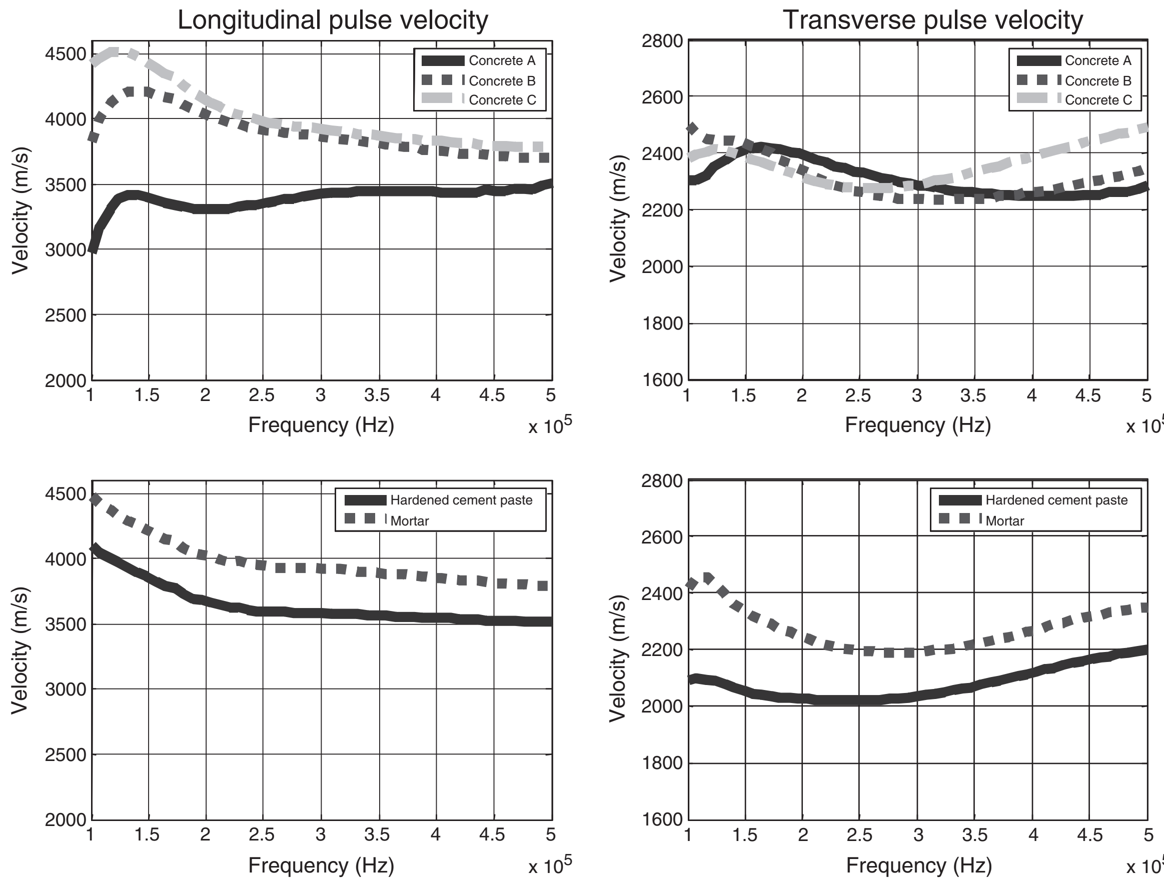

Fig. 7. Frequency-dependent velocity of longitudinal and transverse pulses based on Mexican hat wavelets.

and amplify useless data, such as noise. In CWT-based analysis one should therefore carefully elect the wavelet to be employed.

5.2. Pulse type

The pulse type used in the analysis is also an important issue. Although for several reasons longitudinal pulses are more frequently used in ultrasonic testing of concrete, previous studies indicate that *transverse pulses are more reliable*, for they are less sensitive to coupling imprecision or acoustic properties mismatch of the aggregates. A study on ultrasonic analysis of concrete subjected to mechanical damage due to uniaxial loading showed that both velocity and attenuation are more reliable and consistent parameters in transverse pulses than in longitudinal pulses [4]. In Figs. 6–9 transverse pulse results are quite consistent – following the same trends and having similar values – for hardened cement paste and mortar. Concrete mixes analyzed with transverse pulses – for the reasons explained in previous paragraph – were only consistent when the *slower* wavelets were used: Haar and Mexican hat wavelets (Figs. 6 and 7). Transverse wave velocity curves calculated with Haar and Mexican hat wavelets are grouped, showing minor variations for all three concretes studied.

Results for longitudinal pulses applied to concrete (left top plots in Figs. 6–9) show a spread of results at lower frequencies and a tendency for more uniform velocity values as the frequency increases. This spreading of the velocities at lower frequencies and the tendency to more constant values at higher ones was also reported in the experimental study conducted by Philippidis and Aggelis, who applied narrow band longitudinal pulses of different frequencies to analyze cement-based materials [11]. The more *constant* behavior of the longitudinal velocities at higher frequencies (for all wavelets used) indicates that this range of the spectrum is more reliable to detect changes in the microstructure of cement-based materials. Uniformity of velocities and the fact that changes in microstructure are more likely to influence shorter wavelengths (higher frequencies) lead to this conclusion.

5.3. Mix coarseness

Coarseness of the mixes is another aspect that directly influences the frequency-dependent velocity measurements. As above explained the inquiring wavelengths in the frequency spectrum used for transverse and longitudinal pulses are in the intervals $\lambda_T \in [4.8\text{ mm}, 24\text{ mm}]$ and $\lambda_L \in [8\text{ mm}, 40\text{ mm}]$. Since the grain-sizes in the admixtures vary from cement powder and sand (with less than 1 mm) up to coarse aggregate with a little more than 1 cm (used in mix A), the wavelengths are in *stochastic* and *Rayleigh* attenuating regions. In the results, hardened cement paste and mortar showed – regardless of the wavelet used – the same general aspect, with velocities in hardened paste about 10% lower than in mortar for both transverse and longitudinal waves. The longitudinal velocity of those two mixes also showed less oscillation than the concrete mixes. For the longitudinal pulses propagating in the concrete mixes, the coarser the mix, the slower the propagation in the frequency range considered. In the coarser mix A the pulses were slow, in medium mix B velocity is higher, while in mix C pulses were the fastest. It is also interesting to notice that longitudinal wave propagating in mortar behaves quite similarly to the finest concrete mix C. This happens because both fine concrete and mortar have a large amount of fine aggregates (in both mixes, more than 50% of aggregate weight passes through sieve No. 8 — 2.38 mm). Indeed, with regard to the longitudinal waves, if one looks at the three concretes and mortar as a sequence of mixes of decreasing coarseness (mix A, mix B, mix C, and mortar) the four

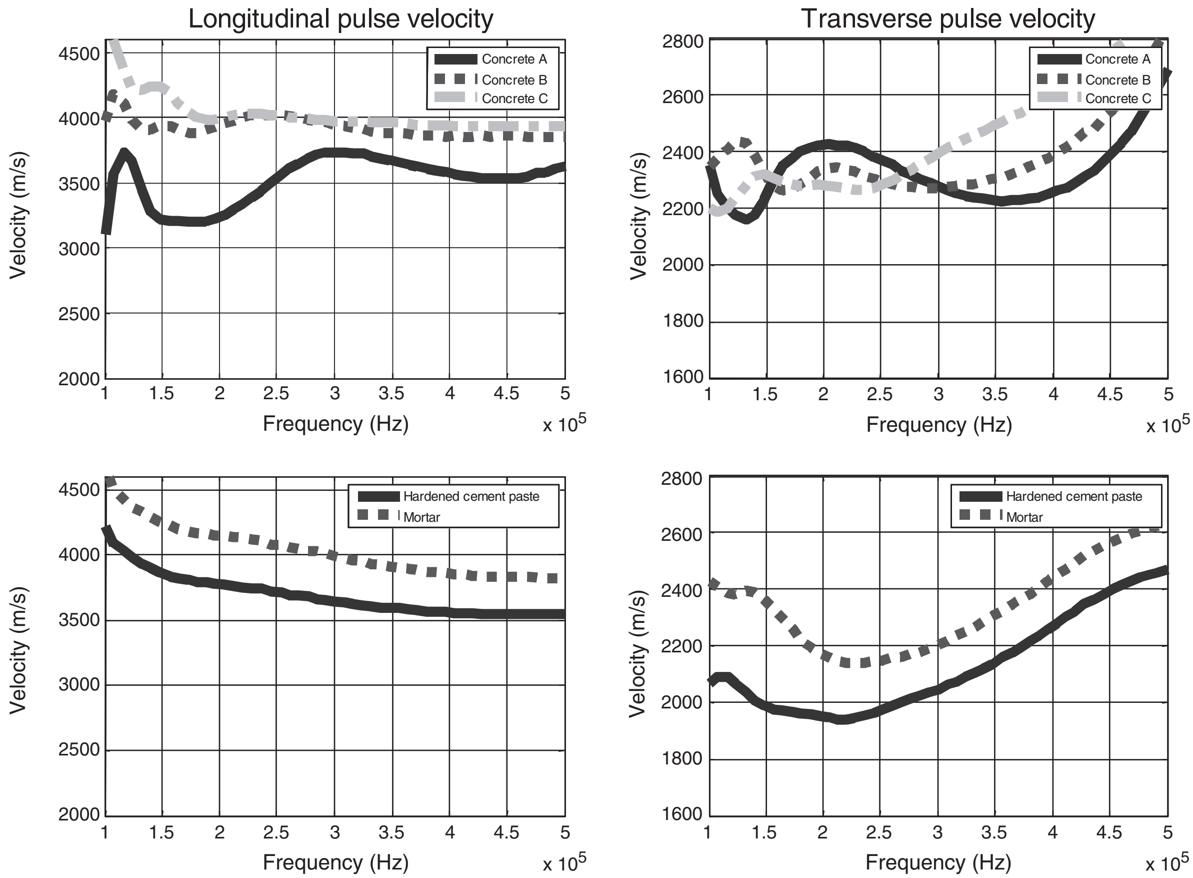

Fig. 8. Frequency-dependent velocity of longitudinal and transverse pulses based on Daubechies 6 wavelets.

velocity curves obtained with *each wavelet type*, considered together show a tendency to an almost constant velocity value as the frequency increases. Consider, for instance, the longitudinal pulse velocities of concretes and mortar in Fig. 6 (Haar wavelet): starting at 2250 m/s mix A has a strong positive slope that decreases as the frequency increases, in mix B the slope – still positive – is not as steep: the dotted curve starts at 3200 m/s and soon becomes constant, mix C – whose curve starts at 3800 m/s – is almost constant in the whole spectrum, and, finally, the mortar mix – following the behavior of concretes – starts (now with a negative slope) at an even higher velocity – 4200 m/s, approximately. It is also worth noticing that while at low frequencies pulse velocity curves of mix B, mix C, and mortar show some spread, as frequency increases velocities of these three materials tend to the same value (mix A showed lower velocities). Figs. 7, 8 and 9 (Mexican hat, Daubechies 6, and Daubechies 10 wavelets, respectively) also show a less oscillating behavior of longitudinal pulse velocities in concrete mixes as frequency increases. Transverse wave velocities, regardless of the wavelet used, did not show any tendency that could be linked to mix coarseness. In Fig. 6, for example, all concrete mixes follow the same behavior and the curves are almost coincident. The same *non sensitivity to mix design* occurs for transverse pulse velocity in the curves calculated with other wavelets. Comparing the results obtained for transverse and longitudinal frequency-dependent wave velocity propagating in concrete and mortar, one can conclude that although transverse wave velocity is more reliable and consistent to measure damage in concrete [4], longitudinal pulse speed is more sensitive to mix design.

The results – considering the three abovementioned aspects: wavelet, pulse type, and coarseness of aggregates used in each mix – clearly indicate the capability of CWT to extract frequency-dependent velocities from single pairs of broadband probes.

6. Conclusions

Continuous wavelet transform (CWT) was applied to ultrasonic pulses to obtain frequency-based information from broadband transducers. In the experimental program transverse and longitudinal pulses with broad frequency spectra were partitioned with CWT-based time-frequency diagrams and frequency-dependent velocities calculated. Using 4 wavelet types (Haar, Mexican hat, Daubechies 6 and Daubechies 10) the method was applied to 5 cementitious materials (three concretes, mortar and hardened cement paste) and frequency-based velocity curves were calculated and analyzed with emphasis on three aspects: wavelet family, propagating pulse type (longitudinal or transverse), and mix coarseness.

From the analysis of the results the first remarkable conclusion is that transverse pulses are less sensitive to grain-size distribution than longitudinal pulses. Wavelengths of the inquiring signals ($\lambda_T \in$[4.8 mm, 24 mm] and $\lambda_L \in$[8 mm, 40 mm]) allowed aggregates to activate both stochastic and Rayleigh attenuating regions. Results showed that – for the wavelengths used – regardless of the wavelet adopted, frequency-dependent velocity curves for transverse waves are grouped for all concrete and mortar mixes. The only mix that did not follow the same trend – showing a slower speed – was hardened cement paste. Frequency-dependent velocity plots also indicated that longitudinal pulses at lower frequencies (from 100 kHz up to 250 kHz) show some dispersion and oscillating behavior. At higher frequencies – between 350 kHz and 500 kHz – longitudinal velocity readings are more stable, indicating that this range of frequencies is adequate to detect microcracks and other diffuse damage. Comparing the results for transverse and longitudinal velocities it can be concluded that although previous results emphasized that transverse waves are more reliable and consistent for mechanical damage analysis [4], longitudinal

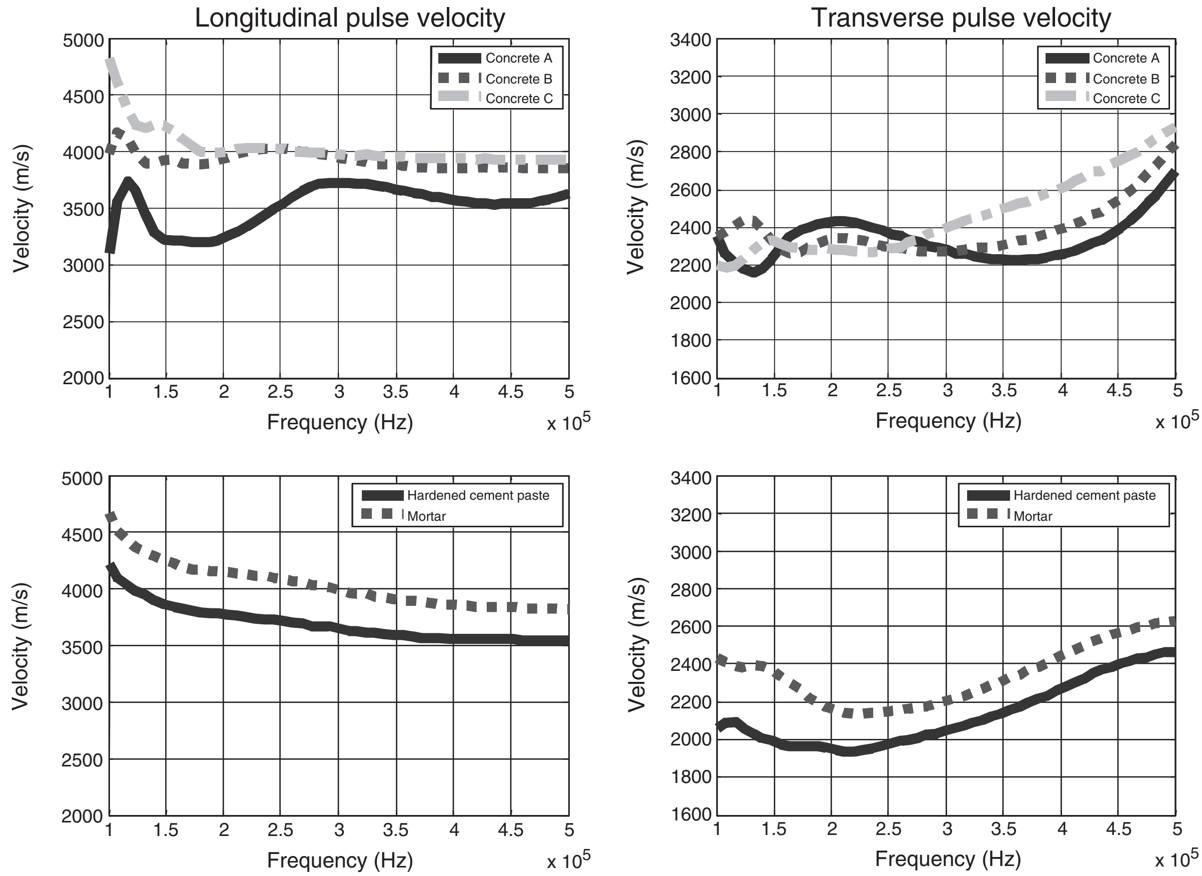

Fig. 9. Frequency-dependent velocity of longitudinal and transverse pulses based on Daubechies 10 wavelets.

waves at lower frequencies are more sensitive to grain size and mix design.

From the velocity curves it became clear that the wavelet type employed in the analysis plays an important role and a poorly-chosen wavelet may lead to wrong results. Spurious results were observed in the curves for transverse wave velocities calculated with faster wavelets (Daubechies 6 and Daubechies 10). The research also showed that the wavelet type can be used as a parameter to be adjusted and to improve the results. When the wavelet family allows wavelets of sequential order to be generated, *wavelet order* can be used as a parameter (such is the case with Daubechies, Symlet and Coiflet wavelets).

With regard to the approach used in the research, capability of CWT to analyze frequency-based velocity of ultrasonic transverse and longitudinal pulses was demonstrated. With the application of wavelets traditional attenuation-based analysis of ultrasound propagation in concrete can be enhanced with approaches based upon frequency-dependent longitudinal and transverse pulse velocity. Frequency-dependent measurements calculated from time-frequency diagrams can also be used in damage detection and mix design characterization. Since cement-based material properties (modulus of elasticity, Poisson's ratio, density, strength) and the degradation of those properties (due to diffuse damage resulting from mechanical damage, freeze and thaw cycles, chemical attack, alkali–silica reaction etc.) can be more easily quantified with velocity measurements than with attenuation, frequency-based pulse velocity analysis is a very useful tool for more sophisticated and complex ultrasonic applications. It is worth emphasizing that although the method presented in this research was used for ultrasonic pulses propagating in cement-based materials, any inspection technique based upon wave propagation, regardless of the wave nature (elastic – transverse or longitudinal – or acoustic) and regardless of its frequency (sonic or ultrasonic) can benefit from CWT-based frequency analysis.

References

[1] J. Leslie, W. Cheesman, Ultrasonic method of studying deterioration and cracking in concrete structures, ACI J. 46 (1) (1949) 17–24.
[2] S.F. Selleck, E.N. Landis, M.L. Peterson, S.P. Shah, J.G. Achenbach, Ultrasonic investigation of concrete with distributed damage, ACI Mater. J. 95 (1) (1998) 27–36.
[3] C.L. Nogueira, Wavelet analysis of ultrasonic pulses in cement-based materials, ACI Mater. J. 107 (3) (2010) 248–257.
[4] C.L. Nogueira, K.J. Willam, Ultrasonic testing of damage in concrete under uniaxial compression, ACI Mater. J. 98 (3) (2001) 265–275.
[5] I. Daubechies, The wavelet transform, time-frequency localization and signal analysis, IEEE Trans. Inf. Theory 36 (5) (1990).
[6] A. Graps, An Introduction to Wavelets, Institute of Electrical and Electronics Engineers, 1995.
[7] M. Misiti, Y. Misity, G. Oppenheim, J.-M. Poggi, Wavelet Toolbox, Wathworks, 1996.
[8] S. Mallat, A Wavelet Tour of Signal Processing, Academic Press, 1998.
[9] G. Strang, T. Nguyen, Wavelets and Filter Banks, Wellesley College, 1996.
[10] P.A. Gaydecki, F.M. Burdekin, W. Damaj, D.G. Johns, P.A. Payne, The propagation and attenuation of medium-frequency ultrasonic waves in concrete: a signal analytical approach, Meas. Sci. Technol. 3 (1992) 126–134.
[11] L.J. Jacobs, J.O. Owino, Effect of aggregate size on attenuations of Rayleigh surface waves in cement-based materials, ASCE J. Eng. Mech. 126 (11) (2000) 1124–1130.
[12] J.O. Owino, L.J. Jacobs, Attenuation measurements in cement-based materials using laser ultrasonics, ASCE J. Eng. Mech. 125 (6) (1999) 637–647.
[13] T.P. Philippidis, D.G. Aggelis, Experimental study of wave dispersion and attenuation in concrete, Ultrasonics 43 (2005) 584–595.
[14] W. Suaris, V. Fernando, Ultrasonic pulse attenuation as a measure of damage growth during cyclic loading of concrete, ACI Mater. J. 84 (3) (1987) 185–193.
[15] D. Nicoletti, N. Bilgutay, B. Onaral, Power-law relationships between the dependence of ultrasonic attenuation on wavelength and the grain size distribution, J. Acoust. Soc. Am. 91 (6) (1992) 32–78.
[16] E.P. Papadakis, Ultrasonic attenuation caused by scattering in polycrystalline metals, J. Acoust. Soc. Am. 37 (4) (1965) 711–717.
[17] E.P. Papadakis, Revised grain-scattering formulas and tables, J. Acoust. Soc. Am. 37 (4) (1965) 703–710.

[18] E.N. Landis, S.P. Shah, Frequency-dependent stress wave attenuation in cement-based materials, ASCE J. Eng. Mech. 121 (6) (1995) 737–743.
[19] Y. Berthaud, Damage measurements concrete via an ultrasonic technique: part I. Experiment, Cem. Concr. Res. (21) (1991) 73–82.
[20] Y. Berthaud, Damage measurements concrete via an ultrasonic technique: part II. Modelling, Cem. Concr. Res. (21) (1991) 219–228.
[21] J. Becker, L.J. Jacobs, J. Qu, Characterization of cement-based materials using diffuse ultrasound, ASCE J. Eng. Mech. 129 (12) (2003) 1478–1484.
[22] A.A. Shah, S. Hirose, Nonlinear ultrasonic investigation of concrete damaged under uniaxial compression step, ASCE J. Mater. In Civ. Engnr. 22 (5) (2010) 476–484.
[23] S. Popovics, N.M. Bilgutay, M. Karaoguz, T. Akgul, High-frequency ultrasound technique for testing concrete, ACI Mater. J. 97 (1) (2000) 58–65.
[24] J.W. Ju, L.-S. Weng, Y. Liu, Ultrasonic frequency-dependent amplitude attenuation characteristics technique for nondestructive evaluation of concrete, ACI Mater. J. 103 (3) (2006) 177–185.
[25] D.G. Aggelis, T. Shiotani, Effect of inhomogeneity parameters on wave propagation in cementitious material, ACI Mater. J. 105 (2) (2008) 187–193.
[26] N. De Belie, C.U. Grosse, J. Kurz, H.-W. Reinhardt, Ultrasound monitoring of the influence of different accelerating admixtures and cement types for shotcrete on setting hardening behaviour, Cem. Concr. Res. (35) (2005) 2087–2094.
[27] N. De Belie, C. Grosse, G. Baert, Ultrasonic transmission to monitor setting and hardening of fly ash concrete, ACI Mater. J. 105 (3) (2008) 221–226.